Bioinformatic prediction of immunodominant regions in spike protein for early diagnosis of the severe acute respiratory syndrome coronavirus 2 (SARS-CoV-2)

Siqi Zhuang [1], **Lingli Tang** [1], **Yufeng Dai** [1], **Xiaojing Feng** [1], **Yiyuan Fang** [1], **Haoneng Tang** [1], **Ping Jiang** [1], **Xiang Wu** [2], **Hezhi Fang** [3], **Hongzhi Chen** [Corresp. 4]

[1] Department of Laboratory Medicine, The Second Xiangya Hospital, Central South University, Changsha, Hunan, China

[2] Department of Parasitology, Xiangya School of Basic Medicine, Central South University, Changsha, Hunan, China

[3] Key Laboratory of Laboratory Medicine, Ministry of Education, Zhejiang Provincial Key Laboratory of Medical Genetics, College of Laboratory Medicine and Life Sciences,, Wenzhou Medical University,, Wenzhou, Zhejiang, China

[4] National Clinical Research Center for Metabolic Disease, Key Laboratory of Diabetes Immunology, Ministry of Education, Metabolic Syndrome Research Center, and Department of Metabolism & Endocrinology, The Second Xiangya Hospital, Central South University, Changsha, Hunan, China

Corresponding Author: Hongzhi Chen
Email address: chenhongzhi2013@csu.edu.cn

Background. To contain the pandemics caused by SARS-CoV-2, early detection approaches with high accuracy and accessibility are critical. Generating an antigen-capture based detection system would be an ideal strategy complementing the current methods based on nucleic acids and antibody detection. The spike protein is found on the outside of virus particles and appropriate for antigen detection.

Methods. In this study, we utilized bioinformatics approaches to explore the immunodominant fragments on spike protein of SARS-CoV-2.

Results. The S1 subunit of spike protein was identified with higher sequence specificity. Three immunodominant fragments, $Spike_{56\text{-}94}$, $Spike_{199\text{-}264}$, and $Spike_{577\text{-}612}$, located at the S1 subunit were finally selected via bioinformatics analysis. The glycosylation sites and high-frequency mutation sites on spike protein were circumvented in the antigen design. All the identified fragments present qualified antigenicity, hydrophilicity, and surface accessibility. A recombinant antigen with a length of 194 amino acids (aa) consisting of the selected immunodominant fragments as well as a universal Th epitope was finally constructed.

Conclusion. The recombinant peptide encoded by the construct contains multiple immunodominant epitopes, which is expected to stimulate a strong immune response in mice and generate qualified antibodies for SARS-CoV-2 detection.

Bioinformatic prediction of immunodominant regions in spike protein for early diagnosis of the severe acute respiratory syndrome coronavirus 2（SARS-CoV-2）

Siqi Zhuang[2], Lingli Tang[2], Yufeng Dai[2], Xiaojing Feng[2], Yiyuan Fang[2], Haoneng Tang[2], Ping Jiang[2], Xiang Wu[3], Hezhi Fang[4], Hongzhi Chen[1]

1. National Clinical Research Center for Metabolic Disease, Key Laboratory of Diabetes Immunology, Ministry of Education, Metabolic Syndrome Research Center, and Department of Metabolism & Endocrinology, The Second Xiangya Hospital, Central South University, Changsha, Hunan 410011, China

2. Department of Laboratory Medicine, The Second Xiangya Hospital, Central South University, Changsha, Hunan 410011, China.

3. Department of Parasitology, Xiangya School of Basic Medicine, Central South University, Changsha, Hunan 410013, China

4. Key Laboratory of Laboratory Medicine, Ministry of Education, Zhejiang Provincial Key Laboratory of Medical Genetics, College of Laboratory Medicine and Life Sciences, Wenzhou Medical University, Wenzhou, Zhejiang 325035, China

Corresponding author:

Hongzhi Chen[1]

E-mail address: chenhongzhi2013@csu.edu.cn

Abstract

Background. To contain the pandemics caused by SARS-CoV-2, early detection approaches with high accuracy and accessibility are critical. Generating an antigen-capture based detection system would be an ideal strategy complementing the current methods based on nucleic acids and antibody detection. The spike protein is found on the outside of virus particles and appropriate for antigen detection.

Methods. In this study, we utilized bioinformatics approaches to explore the immunodominant fragments on spike protein of SARS-CoV-2.

Results. The S1 subunit of spike protein was identified with higher sequence specificity. Three immunodominant fragments, $Spike_{56\text{-}94}$, $Spike_{199\text{-}264}$, and $Spike_{577\text{-}612}$, located at the S1 subunit were finally selected via bioinformatics analysis. The glycosylation sites and high-frequency mutation sites on spike protein were circumvented in the antigen design. All the identified fragments present qualified antigenicity, hydrophilicity, and surface accessibility. A recombinant antigen with a length of 194 amino acids (aa) consisting of the selected immunodominant fragments as well as a universal Th epitope was finally constructed.

Conclusion. The recombinant peptide encoded by the construct contains multiple immunodominant epitopes, which is expected to stimulate a strong immune response in mice and generate qualified antibodies for SARS-CoV-2 detection.

Introduction

The severe acute respiratory syndrome coronavirus 2 (SARS-CoV-2) is highly contagious and has caused more than one hundred million infection cases and over 2.4 million deaths (https://www.who.int/, as of February 15, 2021), posing a huge economic and social burden internationally (Lan et al. 2020; Shang et al. 2020). The reports of SARS-CoV-2 reinfection cases suggest that stronger international efforts are required to prevent COVID-19 re-emergence in the future(Zhan et al. 2020). Nevertheless, the possibility of SARS-CoV-2 becoming a seasonal epidemic cannot be excluded (Shaman & Galanti 2020). Even worse, the large number of asymptomatic infections greatly increase the difficulties of epidemic control(Rothe et al. 2020). At present, no specific drugs have been developed for SARS-CoV-2, and the effectiveness of the vaccines on the market still needs time to be evaluated. Therefore, early detection and isolation of infected people are still indispensable means to control the spread of the epidemic, which requires accurate, early, economical, and easy-to-operate diagnostic methods(Yan et al. 2020).

The real-time reverse transcriptase-polymerase chain reaction(RT-PCR) and antibody-capture serological tests are currently the main diagnostic methods for SARS-CoV-2 (Ishige et al. 2020). As the golden standard, RT-PCR is highly reliable (Bustin & Nolan 2020; Padoan et al. 2020). However, the implementation costs and relatively cumbersome operation problems make it a big challenge for large population screening(Thabet et al. 2020). The antibody-capture serological test is convenient, but seroconversion generally occurs in the second or third week of illness. Therefore, it is not ideal for the early diagnosis of infection (Hachim et al. 2020; Liu et

al. 2020; Tang et al. 2020). The antigen-capture test is an alternative diagnostic method that relies on the immunodetection of viral antigens in clinical samples. Accordingly, this method could be applied for the detection of early infection no matter if the patient was asymptomatic or not (Ohnishi 2008). Compared with RT-PCR based detection method, it is relatively inexpensive and can be used at the point-of-care.

Rapid viral antigen detection has been successfully used for diagnosing respiratory viruses such as influenza and respiratory syncytial viruses (Cazares et al. 2020; Ji et al. 2011; Ohnishi et al. 2005; Ohnishi et al. 2012; Qiu et al. 2005). The sensitivity and specificity of the antigen-capture detection system depend highly on the antigen employed to generate antibodies (Ohnishi et al. 2012). The spike protein is one of the structural proteins of SARS-CoV-2, with the majority located on the outside surface of the viral particles (Fehr & Perlman 2015; Kumar et al. 2020; Woo et al. 2005). It has a 76.4% homology with the spike protein of SARS-CoV. Sunwoo's study showed that the bi-specific spike protein derived monoclonal antibody system exhibited excellent sensitivity in SARS-CoV detection (Sunwoo et al. 2013). The virus infection is initiated by the interaction of spike protein receptor-binding domain (RBD) and angiotensin-converting enzyme 2 (ACE2) on host cells. It is widely accepted that the spike protein is one of the earliest antigenic proteins recognized by the host immune system (Callebaut et al. 1996; Chen et al. 2020c; Gomez et al. 1998; Lu et al. 2004; Sanchez et al. 1999). Nevertheless, the difficulties of using spike protein as an antigen are also obvious. Firstly, it is not easy to express and purify the full-length spike protein (Tan et al. 2004). Besides, the spike protein is highly glycosylated (Kumar et al. 2020) and prone to mutation(Wang et al. 2020a), which may

84 counteract the sensitivity of antigen-capture based detection method. Hence, it is critical to
85 truncating the glycosylation and mutation sites on spike protein as much as possible in antigen
86 design (Meyer et al. 2014; Tan et al. 2004). A study using the truncated spike protein to detect
87 SARS-CoV achieved a diagnostic sensitivity of >99% and a specificity of 100% (Mu et al.
88 2008), which suggests that the truncated spike protein of SARS-CoV-2 could also be an
89 appropriate candidate for the early diagnostic testing and screening of SARS-CoV-2. In this
90 study, we analyzed the spike protein via bioinformatics tools to obtain immunodominant
91 fragments. The predicted sequences were joined together as a novel antigen for the immunization
92 of mice and antibody production. Epitopes information presented by this work may aid in
93 developing a promising antigen-capture based detection system in pandemic surveillance and
94 containment.
95

96 ## Method

97 ## Data retrieval and sequence alignment

98 Multiple bioinformatics analysis tools were used in this study, and the flowchart is depicted
99 in Fig. 1. Coronaviruses had four genera composed of alpha-, beta-, gamma- and delta-
100 coronaviruses. Among them, alpha- and beta- genera could infect humans. Seven beta-
101 coronaviruses are known to infect humans (HCoV-229E, HCoV-OC43, HCoV-NL63, HCoV-
102 HKU1, SARS-CoV, MERS-CoV, and SARS-CoV-2) (Kin et al. 2015; Su et al. 2016). We
103 utilized the NCBI database to obtain the sequences of these human-related coronaviruses spike
104 proteins, of which accession numbers were presented in Fig. 2A. The Clustal Omega Server-

Multiple Sequence Alignment was used to analyze the sequence similarity. The analysis of the phylogenetic tree was calculated by the same server. In this study, we set parameters of Clustal Omega as default (Sievers et al. 2011). Additionally, we conducted the EMBOSS Needle Server-Pairwise Sequence Alignment(Needleman & Wunsch 1970) to compare the whole sequence and several major domains between SARS-CoV-2 and SARS-CoV to find out the specific genomic regions on SARS-CoV-2.

Linear B-cell epitope prediction

Linear B-cell epitopes of the SARS-CoV-2 spike protein were calculated by ABCpred and Bepipred v2.0 servers. For ABCpred, we set a threshold of 0.8 to achieve a specificity of 95.50% and an accuracy of 65.37% for prediction. The window length was set to 16 (the default window length) in this study (Saha & Raghava 2006). The BepiPred v2.0 combines a hidden Markov model and a propensity scale method. The score threshold for the BepiPred v2.0 was set to 0.5(the default value) to obtain a specificity of 57.16% and a sensitivity of 58.56% (Jespersen et al. 2017). The residues with scores above 0.5 were predicted to be part of an epitope.

T-cell epitope prediction

The free online service TepiTool server, integrated into the Immune Epitope Database (IEDB), was used to forecast epitopes binding to mice MHC molecules(Paul et al. 2016). Alleles including H-2-Db, H-2-Dd, H-2-Kb, H-2-Kd, H-2-Kk, and H-2-Ld were selected for MHC-I binding epitopes analysis. We checked the “IEDB recommended” option during computation and

126 retained sequences with predicted consensus percentile rank ≤1 as predicted epitope(Trolle et al.
127 2015). For MHC-II binding epitopes, alleles including H2-IAb, H2-IAd, and H2-IEd were
128 selected for analysis. As the same as MHC-I binding computation, we chose the "IEDB
129 recommended" option, and peptides with predicted consensus percentile rank ≤10 were
130 identified as potential epitopes(Wang et al. 2010; Zhang et al. 2012).
131

132 Profiling and evaluation of selected fragments

133 The secondary structure of the SARS-CoV-2 spike protein (PDB ID: 6VSB chain B) was
134 calculated by the PyMOL molecular graphics system using the SSP algorithm. PyMOL
135 (http://www.pymol.org) is a python-based tool, which is widely used for visualization of
136 macromolecules, such as SARS-CoV-2 spike protein in the current study (Yuan et al. 2016).
137 Vaxijen2.0 server was utilized to analyze the antigenicity of epitopes and selected fragments. A
138 default threshold of 0.4 was set and the prediction accuracy is between 70% and 89%
139 (Doytchinova & Flower 2007). The hydrophilicity of the selected fragment was analyzed by the
140 online server ProtScale (Wilkins et al. 1999). Surface accessibility of predicted fragments was
141 evaluated by NetsurfP, an online server calculating the surface accessibility and secondary
142 structure of amino acid sequence (Petersen et al. 2009). Critical features such as allergenicity and
143 toxicity were evaluated by online server AllerTOP v2.0 (Dimitrov et al. 2014) and ToxinPred
144 (Gupta et al. 2013). In addition, we utilized IEDB (www.iedb.org) to search the selected
145 fragments and epitopes to clarify whether these peptides have been experimentally verified(Vita
146 et al. 2019). Protein sequence BLAST was performed to evaluate the possibility of cross-

reactivity with other mouse protein sequences(Altschul et al. 1997).

Results

Sequence alignment of spike protein in different coronaviruses

We performed sequence alignment to determine the evolutionary relationships between SARS-CoV-2 and other beta-coronaviruses that could infect humans. According to the results of sequence alignment (Fig. 2A, Fig. 2B), SARS-CoV is the closest virus to SARS-CoV-2 among the seven HCoVs, exhibiting a 77.46% sequence identity. To better understand the divergence of spike protein sequences between SARS-CoV-2 and SARS-CoV, we further analyzed the sequences of main domains. Results showed that the S2 subunit was the most conserved domain with a 90.0% identity. RBM and NTD domains, which were located in the S1 subunit, exhibited 49.3% and 50.0% identity respectively (Fig. 2C, Fig. 2D). Hence, we chose the S1 subunit (amino acid 1-685) for the subsequent bioinformatics analysis given their high specificity.

Linear B-cell epitope prediction of S1 subunit in SARS-CoV-2 spike protein

The B-cell epitope is a surface accessible cluster of amino acids, which could be recognized by secreted antibodies or B-cell receptors and elicit humoral immune response (Getzoff et al. 1988). The immunodominant fragments should contain high-quality linear B-cell epitopes to stimulate antibody production effectively. The sequence of the SARS-CoV-2 S1 subunit was evaluated via ABCpred and BepiPred v2.0. A total of 31 peptides were identified by

the ABCpred algorithm (Table S1). For the Bepipred v2.0 server, 14 epitopes were forecasted (Table S2). After antigenicity evaluation, 19 and 9 potential linear B-cell epitopes predicted by the ABCpred server and BepiPred v2.0 server were obtained respectively (Table 1). The peptides predicted by both bioinformatics programs are more likely to be an epitope recognized *in vivo*. After mapping the positions of peptides identified by these servers, 3 regions containing predicted epitopes were obtained. These regions could be preliminarily considered as candidates for immunodominant fragments (Fig.3, Table 2).

Murine T-cell epitope prediction of S1 subunit in SARS-CoV-2 spike protein

Though B cells are responsible for producing antibodies, humoral immunity is heavily dependent on the activation of T cells (Cho et al. 2019a). Helper T cells (Th) recognize antigen peptides presented by MHC-II molecules and facilitate the humoral immune response (Cho et al. 2019b; Mahon et al. 1995). During humoral immune responses, antigen-activated T cells could provide help in many aspects including directing antibody class switching and guiding the differentiation of antibody-secreting plasma cells as well as the properties of the B-cell antigen receptor(Cho et al. 2019a; Paus et al. 2006; Shulman et al. 2014). Therefore, the immunodominant fragments containing T-cell epitopes could offer essential help to powerful antibody production. The S1 subunit was selected for the prediction of T-cell epitopes. We utilized the TepiTool server to forecast MHC-I and MHC-II binding epitopes. A total of 35 MHC-I binding epitopes was predicted (Table S3), and 27 peptides were identified as MHC-II

189 binding epitopes (Table S4). The antigenicity of these peptides was calculated via Vaxijen 2.0
190 server (Table 3). Combined with the MHC-II epitopes prediction results, the candidate
191 immunodominant fragments were adjusted (Fig.4). Compared with the preliminary candidate
192 immunodominant fragments screened according to the linear B-cell epitope prediction, we added
193 the $Spike_{14-34}$ fragment into consideration because it contains a linear B epitope and an MHC-II
194 binding epitope, both of which had high antigenicity scores (Table 4).
195

196 Immunodominant fragments refinement according to the
197 glycosylation site distribution, mutation site distribution, and
198 secondary structure

199 A profile of 24 glycosylation sites of SARS-CoV-2 spike protein has been reported
200 (Shajahan et al. 2020). Since glycans could hinder the recognition of antigens by shielding the
201 residues (Walls et al. 2019), protein glycosylation would affect the performance of antigen
202 detection. Thus, glycosylation sites should be circumvented when selecting the immunodominant
203 fragments. According to the study of Asif Shajahan et al, 15 glycosylation sites were located in
204 the S1 subunit of the spike protein(Shajahan et al. 2020). Hence, the fragments in this study were
205 adjusted to $Spike_{14-34}$, $Spike_{49-101}$, $Spike_{199-261}$, and $Spike_{583-620}$. To retain antigenicity of the
206 epitopes, the final identified fragments only contained 3 glycosylation sites which should have a
207 minimum effect on antigen recognition.
208 Rapid transmission of COVID-19 provides the SARS-CoV-2 with substantial opportunities
209 for natural selection and mutations. To ensure the stability of the detection method, the

immunodominant fragments were modified to avoid high-frequency mutation sites(Wang et al. 2020b). $Spike_{14-34}$ were excluded for containing four high-frequency mutation sites. Fragment $Spike_{49-101}$ was adjusted to $Spike_{56-92}$, and fragment $Spike_{583-620}$ was adjusted to $Spike_{583-609}$. By adjusting the fragments, we avoided in a total of 8 high-frequency mutation sites (L5F, L18F, T29I, R21K/T, H49Y, L54F, S98F, D614G). The mainly mutant sites on the recent emergent highly infectious variants (including B.1.1.7, B.1.351, and P.1), such as N501Y, D614G, E484K, Y144del, K417N, and A570D were also not included in our fragments. The adjusted fragments contain none of the above high-frequency mutation sites, which might avoid the impact of mutations on detection performance and improve the detection efficiency in the future(Li et al. 2020; Tegally et al. 2020).

The PyMOL was used to present the secondary structure of the spike protein (PDB ID: 6VSB）(Fig. S1). To keep the integrity of the secondary structure of the selected fragments, we extended the N- and C- ends with 2~5 residues, and the immunodominant fragments were finally adjusted to $Spike_{56-94}$, $Spike_{199-264}$, and $Spike_{577-612}$. The epitopes and potential glycosylation sites contained in the selected immunodominant fragments were displayed in Fig. 5.

Profiling, evaluation, and visualization of selected immunodominant fragments

To further evaluate the antibody binding potentiality of these antigenic regions, the key features of the selected fragments such as antigenicity, hydrophilicity, surface accessibility, toxicity, and allergenicity were analyzed and presented (Table 5). The hydrophilicity and surface

accessibility of the spike protein subunit 1 were calculated. The selected fragments of interest were submitted for computation of antigenicity, toxicity, and allergenicity. Three fragments presented relatively moderate hydrophilicity and surface accessibility. The proportion of hydrophilic amino acids in the selected fragments $Spike_{56-94}$, $Spike_{199-264}$, $Spike_{577-612}$ are 48.72%, 45.45%, 33.33% respectively. The surface accessibility of these fragments calculated by the online server was shown in Table 5.

The toxicity of the selected fragments was examined and no fragment was predicted to be toxic. The allergenicity was assessed and only fragment $Spike_{577-612}$ was predicted to be a probable allergen. Attention should be paid to monitor potential allergic reactions when injecting the recombinant protein into mice. And the selected fragments were presented as the sphere in the trimer structure (Fig. 6). Next, we scanned the selected fragments utilizing the IEDB database to determine whether they were experimentally tested. The results showed that $Spike_{200-215}$(IEDB ID: 1330367) and $Spike_{238-252}$ (IEDB ID: 1329417) were identified experimentally as HLA class II epitope in SARS-CoV-2. $Spike_{84-92}$ (IEDB ID: 1321049) and $Spike_{202-210}$ (IEDB ID: 1319559) have been experimentally proved as HLA-B epitopes. (Table S5). These findings enhanced the credibility of the current in silico analysis. The fragments identified would have a strong capacity in stimulating powerful antibody production.

Immunodominant fragments based recombinant antigen design

Three immunodominant fragments embody several linear B-cell epitopes, MHC-I binding, and MHC-II binding T-cell epitopes were selected. As a universal Th epitope, the PAN DR

252 epitope [PADRE(AKFVAAWTLKAAA)] was added into the construction aiming to boost
253 helper T cell activity (Alexander et al. 2000; Ghaffari-Nazari et al. 2015). $(GGGGS)_n$ is a wildly
254 used flexible linker with the function of segmenting protein fragments, maintaining protein
255 conformation, preserving biological activity, and promoting protein expression (Chen et al.
256 2013). Finally, we combined the fragments and a PADRE epitope by linker peptide $(GGGGS)_2$
257 and $(GGGGS)_3$ (Chen et al. 2013)(Fig. 7). The predicted antigenicity of the final construct (194
258 aa) was 0.5690 (Table 6). A protein BLAST for the final construct was conducted to evaluate the
259 possibility of cross-reactivity. The BLAST result suggested that, except for the SARS-CoV-2
260 spike protein, no protein would cross-react with the construct (Raw data in the Supplemental
261 Files), which indicated that our fragments possess good specificity.
262

263 Discussion

264 In this study, the immunodominant fragments within the S1 subunit of the SARS-CoV-2
265 spike protein were explored. The final construct consists of three immunodominant fragments
266 $Spike_{56\text{-}94}$, $Spike_{199\text{-}264}$, $Spike_{577\text{-}612}$, and a PADRE epitope. The recombinant antigen will be used
267 to immunize mice to generate qualified antibody which could be applied for developing an
268 antigen-capture based detection system.
269 The antibody-based antigen capturing method is user-friendly, time-saving, and economical.
270 Thus, it is an ideal complementary detection strategy especially for early diagnosis and large
271 population screening. The monoclonal antibodies against SARS-CoV have been successfully
272 applied in the immunological antigen-detection of SARS-CoV (Ohnishi 2008). Accordingly, we

explored the immunodominant fragments on the spike protein of SARS-CoV-2, which would provide aid in developing an accurate and fast antigen-capture based early detection system for SARS-CoV-2.

We selected the S1 subunit for immunodominant fragments screening after divergence analysis. It had been reported that an S1 antigen-based assay of SARS-CoV could capture the virus as soon as the infection occurs (Sunwoo et al. 2013). Jong-Hwan Lee *et al.* designed a method that could seize and detect spike protein S1 subunit of SARS-CoV-2 using ACE2 receptor and S1-mAb(Lee et al. 2021). This finding suggests that it is appropriate to use the S1 subunit for specific and early diagnosis of SARS-CoV-2. Three immunodominant fragments ($Spike_{56-94}$, $Spike_{199-264}$, and $Spike_{577-612}$) were identified in the present study. These sequences will be joined to construct recombinant peptides in the next step. Instead of using inactivated full-length spike protein, we designed a novel recombinant protein construct that increased sequence specificity as well as circumvented mutation sites and glycosylation sites. As the antigen design is based on bioinformatics study, the exact ability of the selected fragments to produce qualified antibodies for virus detection has yet to be determined by experiments.

Noticeably, the spike protein of SARS-CoV-2 is heavily glycosylated. Glycans could shield epitopes during antibody recognition, which may interfere with the detection of viral proteins (Shajahan et al. 2020). About 17 N-glycosylation sites along with two O-glycosylation sites were found occupied in the spike protein of SARS-CoV-2(Shajahan et al. 2020). We circumnavigated most glycosylation sites when selecting immunodominant fragments. The three selected fragments in this study only contain 3 glycosylation sites. In case these glycosylation sites

294 impede the diagnostic performance, an additional deglycosylation step with N-glycanase should
295 be applied for the test specimens (Dermani et al. 2019), which is a simple and efficient method
296 for deglycosylation (Hirani et al. 1987; Huang et al. 2015; Lattová et al. 2016; Zheng et al.
297 2011). Alternatively, an eukaryotic expressing system could be employed to mimic the antigen
298 presented in human cells.

299 Though coronaviruses can find and repair errors during the replication process (Wang et al.
300 2020b), the SARS-CoV-2 genome still presents a large number of mutations. Mutations could
301 not only help virus slip past our immune defense, but also spoil the efficiency of diagnostic tests
302 (Chen et al. 2020b). In this study, we circumvented high-frequency mutation sites when selecting
303 antigen fragments. In addition, our fragments also avoided RBD regions which are prone to
304 mutation (Chen et al. 2020b). The construct finally built contained no high-frequency mutation.

305 To date, several studies using predictive algorithms to analyze SARS-CoV-2 have been
306 reported(Alam et al. 2020; Behmard et al. 2020; Can et al. 2020; Chen et al. 2020a; Dong et al.
307 2020; Poran et al. 2020; Saha et al. 2021; Sohail et al. 2021). However, most of these
308 bioinformatics analyses against SARS-CoV-2 intended to develop effective vaccines to prevent
309 infection and the identified sequences possess high homology with other viruses, especially
310 SARS-CoV (Bhattacharya et al. 2020; Chen et al. 2020a; Robson 2020). On the contrary, the
311 fragments suitable for diagnosis should be unique when compared with other species to ensure
312 the specificity of detection. Therefore, the results obtained from vaccine studies are not ideal for
313 virus detection. In this study, attention was paid to the sequences with high variability, hence the
314 immunodominant fragments identified are more specific. Distinct from vaccine studies, murine

MHC alleles were selected in epitopes prediction in this study, so that the designed antigen could trigger a strong humoral immune response in mice. Furthermore, glycosylated sites and recently identified high-frequency mutation sites were deliberately avoided during the screening process to eliminate their potential adverse impact.

In silico analysis has been widely used to mine and identify various pathogens as well as epitopes prediction (Kiyotani et al. 2020; Liò & Goldman 2004; Qin et al. 2003; Robson 2020; Shen et al. 2003). In this study, identified fragments were further scanned in the IEDB database, and found four peptides contained in the sequences were experimentally validated epitopes (Table S5), which reinforced the conclusion of the present study. In the following studies, we will immunize Balb/c mice with the designed antigen to generate mAbs which could be utilized for SARS-CoV-2 diagnosis after evaluating their sensitivity, specificity, and other related properties.

Conclusion

Through bioinformatics analysis, three immunodominant fragments were identified in the present study. After connected by flexible linkers, we acquired a final recombinant peptide with 194 residues. It was predicted to possess high antigenicity and specificity for SARS-CoV-2. Our next move is to express and purify the recombinant protein in a suitable expression system, followed by immunizing the mice with purified immunogen to obtain specific antibodies. The present study would provide aid in developing an antigen-capture based detection system.

Reference

Alam A, Khan A, Imam N, Siddiqui M, Waseem M, Malik M, and Ishrat R. 2020. Design of an epitope-based peptide vaccine against the SARS-CoV-2: a vaccine-informatics approach. *Briefings in bioinformatics*. 10.1093/bib/bbaa340

Alexander J, del Guercio MF, Maewal A, Qiao L, Fikes J, Chesnut RW, Paulson J, Bundle DR, DeFrees S, and Sette A. 2000. Linear PADRE T helper epitope and carbohydrate B cell epitope conjugates induce specific high titer IgG antibody responses. *J Immunol* 164:1625-1633. 10.4049/jimmunol.164.3.1625

Altschul SF, Madden TL, Schäffer AA, Zhang J, Zhang Z, Miller W, and Lipman DJ. 1997. Gapped BLAST and PSI-BLAST: a new generation of protein database search programs. *Nucleic Acids Res* 25:3389-3402. 10.1093/nar/25.17.3389

Behmard E, Soleymani B, Najafi A, and Barzegari E. 2020. Immunoinformatic design of a COVID-19 subunit vaccine using entire structural immunogenic epitopes of SARS-CoV-2. *Scientific reports* 10:20864. 10.1038/s41598-020-77547-4

Bhattacharya M, Sharma AR, Patra P, Ghosh P, Sharma G, Patra BC, Lee SS, and Chakraborty C. 2020. Development of epitope-based peptide vaccine against novel coronavirus 2019 (SARS-COV-2): Immunoinformatics approach. *J Med Virol* 92:618-631. 10.1002/jmv.25736

Bustin SA, and Nolan T. 2020. RT-qPCR Testing of SARS-CoV-2: A Primer. *Int J Mol Sci* 21. 10.3390/ijms21083004

Callebaut P, Enjuanes L, and Pensaert M. 1996. An adenovirus recombinant expressing the spike glycoprotein of porcine respiratory coronavirus is immunogenic in swine. *J Gen Virol* 77 (Pt 2):309-313. 10.1099/0022-1317-77-2-309

Can H, Köseoğlu AE, Erkunt Alak S, Güvendi M, Döşkaya M, Karakavuk M, Gürüz AY, and Ün C. 2020. In silico discovery of antigenic proteins and epitopes of SARS-CoV-2 for the development of a vaccine or a diagnostic approach for COVID-19. *Sci Rep* 10:22387. 10.1038/s41598-020-79645-9

Cazares LH, Chaerkady R, Samuel Weng SH, Boo CC, Cimbro R, Hsu HE, Rajan S, Dall'Acqua W, Clarke L, Ren K, McTamney P, Kallewaard-LeLay N, Ghaedi M, Ikeda Y, and Hess S. 2020. Development of a Parallel Reaction Monitoring Mass Spectrometry Assay for the Detection of SARS-CoV-2 Spike Glycoprotein and Nucleoprotein. *Anal Chem* 92:13813-13821. 10.1021/acs.analchem.0c02288

Chen HZ, Tang LL, Yu XL, Zhou J, Chang YF, and Wu X. 2020a. Bioinformatics analysis of epitope-based vaccine design against the novel SARS-CoV-2. *Infect Dis Poverty* 9:88. 10.1186/s40249-020-00713-3

Chen J, Wang R, Wang M, and Wei GW. 2020b. Mutations Strengthened SARS-CoV-2 Infectivity. *J Mol Biol* 432:5212-5226. 10.1016/j.jmb.2020.07.009

Chen J, Zhu H, Horby PW, Wang Q, Zhou J, Jiang H, Liu L, Zhang T, Zhang Y, Chen X, Deng X, Nikolay B, Wang W, Cauchemez S, Guan Y, Uyeki TM, and Yu H. 2020c. Specificity, kinetics and longevity of antibody responses to avian influenza A(H7N9) virus infection in humans. *J Infect* 80:310-319. 10.1016/j.jinf.2019.11.024

Chen X, Zaro JL, and Shen WC. 2013. Fusion protein linkers: property, design and functionality. *Adv Drug Deliv Rev* 65:1357-1369. 10.1016/j.addr.2012.09.039

Cho S, Raybuck A, Blagih J, Kemboi E, Haase V, Jones R, and Boothby M. 2019a. Hypoxia-inducible factors in CD4 T cells promote metabolism, switch cytokine secretion, and T cell help in humoral immunity. *Proceedings of the National Academy of Sciences of the United States of America* 116:8975-8984. 10.1073/pnas.1811702116

Cho SH, Raybuck AL, Blagih J, Kemboi E, Haase VH, Jones RG, and Boothby MR. 2019b. Hypoxia-inducible factors in CD4(+) T cells promote metabolism, switch cytokine secretion, and T cell help in humoral immunity. *Proc Natl Acad Sci U S A* 116:8975-8984. 10.1073/pnas.1811702116

Dermani FK, Samadi P, Rahmani G, Kohlan AK, and Najafi R. 2019. PD-1/PD-L1 immune checkpoint: Potential target for cancer therapy. *J Cell Physiol* 234:1313-1325. 10.1002/jcp.27172

Dimitrov I, Bangov I, Flower DR, and Doytchinova I. 2014. AllerTOP v.2--a server for in silico prediction of allergens. *J Mol Model* 20:2278. 10.1007/s00894-014-2278-5

Dong R, Chu Z, Yu F, and Zha Y. 2020. Contriving Multi-Epitope Subunit of Vaccine for COVID-19: Immunoinformatics Approaches. *Frontiers in immunology* 11:1784. 10.3389/fimmu.2020.01784

Doytchinova IA, and Flower DR. 2007. VaxiJen: a server for prediction of protective antigens, tumour antigens and subunit vaccines. *BMC Bioinformatics* 8:4. 10.1186/1471-2105-8-4

Fehr AR, and Perlman S. 2015. Coronaviruses: an overview of their replication and pathogenesis. *Methods Mol Biol* 1282:1-23. 10.1007/978-1-4939-2438-7_1

Getzoff ED, Tainer JA, Lerner RA, and Geysen HM. 1988. The chemistry and mechanism of antibody binding to protein antigens. *Adv Immunol* 43:1-98. 10.1016/s0065-2776(08)60363-6

Ghaffari-Nazari H, Tavakkol-Afshari J, Jaafari MR, Tahaghoghi-Hajghorbani S, Masoumi E, and Jalali SA. 2015. Improving Multi-Epitope Long Peptide Vaccine Potency by Using a Strategy that Enhances CD4+ T Help in BALB/c Mice. *PLoS One* 10:e0142563. 10.1371/journal.pone.0142563

Gomez N, Carrillo C, Salinas J, Parra F, Borca MV, and Escribano JM. 1998. Expression of immunogenic glycoprotein S polypeptides from transmissible gastroenteritis coronavirus in transgenic plants. *Virology* 249:352-358. 10.1006/viro.1998.9315

Gupta S, Kapoor P, Chaudhary K, Gautam A, Kumar R, Open Source Drug Discovery C, and Raghava GP. 2013. In silico approach for predicting toxicity of peptides and proteins. *PLoS One* 8:e73957. 10.1371/journal.pone.0073957

Hachim A, Kavian N, Cohen CA, Chin AWH, Chu DKW, Mok CKP, Tsang OTY, Yeung YC, Perera R, Poon LLM, Peiris JSM, and Valkenburg SA. 2020. ORF8 and ORF3b antibodies are accurate serological markers of early and late SARS-CoV-2 infection. *Nat Immunol* 21:1293-1301. 10.1038/s41590-020-0773-7

Hirani S, Bernasconi RJ, and Rasmussen JR. 1987. Use of N-glycanase to release asparagine-linked oligosaccharides for structural analysis. *Anal Biochem* 162:485-492. 10.1016/0003-2697(87)90424-6

Huang J, Wan H, Yao Y, Li J, Cheng K, Mao J, Chen J, Wang Y, Qin H, Zhang W, Ye M, and Zou H. 2015. Highly Efficient Release of Glycopeptides from Hydrazide Beads by Hydroxylamine Assisted PNGase F Deglycosylation for N-Glycoproteome Analysis. *Anal Chem* 87:10199-10204. 10.1021/acs.analchem.5b02669

Ishige T, Murata S, Taniguchi T, Miyabe A, Kitamura K, Kawasaki K, Nishimura M, Igari H, and Matsushita K. 2020. Highly sensitive detection of SARS-CoV-2 RNA by multiplex rRT-PCR for molecular diagnosis of COVID-19 by clinical laboratories. *Clin Chim Acta* 507:139-142. 10.1016/j.cca.2020.04.023

Jespersen MC, Peters B, Nielsen M, and Marcatili P. 2017. BepiPred-2.0: improving sequence-based B-cell epitope prediction using conformational epitopes. *Nucleic Acids Res* 45:W24-W29. 10.1093/nar/gkx346

Ji Y, Guo W, Zhao L, Li H, Lu G, Wang Z, Wang G, Liu C, and Xiang W. 2011. Development of an antigen-capture ELISA for the detection of equine influenza virus nucleoprotein. *J Virol Methods* 175:120-124. 10.1016/j.jviromet.2011.04.016

Kin N, Miszczak F, Lin W, Gouilh MA, Vabret A, and Consortium E. 2015. Genomic Analysis of 15 Human Coronaviruses OC43 (HCoV-OC43s) Circulating in France from 2001 to 2013 Reveals a High Intra-Specific Diversity with New Recombinant Genotypes. *Viruses* 7:2358-2377. 10.3390/v7052358

Kiyotani K, Toyoshima Y, Nemoto K, and Nakamura Y. 2020. Bioinformatic prediction of potential T cell epitopes for SARS-Cov-2. *J Hum Genet* 65:569-575. 10.1038/s10038-020-0771-5

Kumar S, Maurya VK, Prasad AK, Bhatt MLB, and Saxena SK. 2020. Structural, glycosylation and antigenic variation between 2019 novel coronavirus (2019-nCoV) and SARS coronavirus (SARS-CoV). *Virusdisease* 31:13-21. 10.1007/s13337-020-00571-5

Lan J, Ge J, Yu J, Shan S, Zhou H, Fan S, Zhang Q, Shi X, Wang Q, Zhang L, and Wang X. 2020. Structure of the SARS-CoV-2 spike receptor-binding domain bound to the ACE2 receptor. *Nature*. 10.1038/s41586-020-2180-5

Lattová E, Bryant J, Skřičková J, Zdráhal Z, and Popovič M. 2016. Efficient Procedure for N-Glycan Analyses and Detection of Endo H-Like Activity in Human Tumor Specimens. *J Proteome Res* 15:2777-2786. 10.1021/acs.jproteome.6b00346

Lee JH, Choi M, Jung Y, Lee SK, Lee CS, Kim J, Kim J, Kim NH, Kim BT, and Kim HG. 2021. A novel rapid detection for SARS-CoV-2 spike 1 antigens using human angiotensin converting enzyme 2 (ACE2). *Biosens Bioelectron* 171:112715. 10.1016/j.bios.2020.112715

Li Q, Wu J, Nie J, Zhang L, Hao H, Liu S, Zhao C, Zhang Q, Liu H, Nie L, Qin H, Wang M, Lu Q, Li X, Sun Q, Liu J, Zhang L, Li X, Huang W, and Wang Y. 2020. The Impact of Mutations in SARS-CoV-2 Spike on Viral Infectivity and Antigenicity. *Cell* 182:1284-1294.e1289. 10.1016/j.cell.2020.07.012

Liò P, and Goldman N. 2004. Phylogenomics and bioinformatics of SARS-CoV. *Trends Microbiol* 12:106-111. 10.1016/j.tim.2004.01.005

Liu W, Liu L, Kou G, Zheng Y, Ding Y, Ni W, Wang Q, Tan L, Wu W, Tang S, Xiong Z, and Zheng S. 2020. Evaluation of Nucleocapsid and Spike Protein-based ELISAs for detecting antibodies against SARS-CoV-2. *J Clin Microbiol*. 10.1128/JCM.00461-20

Lu L, Manopo I, Leung BP, Chng HH, Ling AE, Chee LL, Ooi EE, Chan SW, and Kwang J. 2004. Immunological characterization of the spike protein of the severe acute respiratory syndrome coronavirus. *J Clin Microbiol* 42:1570-1576. 10.1128/jcm.42.4.1570-1576.2004

Mahon BP, Katrak K, Nomoto A, Macadam AJ, Minor PD, and Mills KH. 1995. Poliovirus-specific CD4+ Th1 clones with both cytotoxic and helper activity mediate protective humoral immunity against a lethal poliovirus infection in transgenic mice expressing the human poliovirus receptor. *J Exp Med* 181:1285-1292. 10.1084/jem.181.4.1285

Meyer B, Drosten C, and Muller MA. 2014. Serological assays for emerging coronaviruses: challenges and pitfalls. *Virus Res* 194:175-183. 10.1016/j.virusres.2014.03.018

Mu F, Niu D, Mu J, He B, Han W, Fan B, Huang S, Qiu Y, You B, and Chen W. 2008. The expression and antigenicity of a truncated spike-nucleocapsid fusion protein of severe acute respiratory syndrome-associated coronavirus. *BMC Microbiol* 8:207. 10.1186/1471-2180-8-207

Needleman SB, and Wunsch CD. 1970. A general method applicable to the search for similarities in the amino acid sequence of two proteins. *J Mol Biol* 48:443-453. 10.1016/0022-2836(70)90057-4

Ohnishi K. 2008. Establishment and characterization of monoclonal antibodies against SARS coronavirus. *Methods Mol Biol* 454:191-203. 10.1007/978-1-59745-181-9_15

Ohnishi K, Sakaguchi M, Kaji T, Akagawa K, Taniyama T, Kasai M, Tsunetsugu-Yokota Y, Oshima M, Yamamoto K,

Takasuka N, Hashimoto S, Ato M, Fujii H, Takahashi Y, Morikawa S, Ishii K, Sata T, Takagi H, Itamura S, Odagiri T, Miyamura T, Kurane I, Tashiro M, Kurata T, Yoshikura H, and Takemori T. 2005. Immunological detection of severe acute respiratory syndrome coronavirus by monoclonal antibodies. *Jpn J Infect Dis* 58:88-94.

Ohnishi K, Takahashi Y, Kono N, Nakajima N, Mizukoshi F, Misawa S, Yamamoto T, Mitsuki YY, Fu S, Hirayama N, Ohshima M, Ato M, Kageyama T, Odagiri T, Tashiro M, Kobayashi K, Itamura S, and Tsunetsugu-Yokota Y. 2012. Newly established monoclonal antibodies for immunological detection of H5N1 influenza virus. *Jpn J Infect Dis* 65:19-27.

Padoan A, Cosma C, Sciacovelli L, Faggian D, and Plebani M. 2020. Analytical performances of a chemiluminescence immunoassay for SARS-CoV-2 IgM/IgG and antibody kinetics. *Clin Chem Lab Med*. 10.1515/cclm-2020-0443

Paul S, Sidney J, Sette A, and Peters B. 2016. TepiTool: A Pipeline for Computational Prediction of T Cell Epitope Candidates. *Curr Protoc Immunol* 114:18 19 11-18 19 24. 10.1002/cpim.12

Paus D, Phan T, Chan T, Gardam S, Basten A, and Brink R. 2006. Antigen recognition strength regulates the choice between extrafollicular plasma cell and germinal center B cell differentiation. *The Journal of experimental medicine* 203:1081-1091. 10.1084/jem.20060087

Petersen B, Petersen TN, Andersen P, Nielsen M, and Lundegaard C. 2009. A generic method for assignment of reliability scores applied to solvent accessibility predictions. *BMC Struct Biol* 9:51. 10.1186/1472-6807-9-51

Poran A, Harjanto D, Malloy M, Arieta C, Rothenberg D, Lenkala D, van Buuren M, Addona T, Rooney M, Srinivasan L, and Gaynor R. 2020. Sequence-based prediction of SARS-CoV-2 vaccine targets using a mass spectrometry-based bioinformatics predictor identifies immunogenic T cell epitopes. *Genome medicine* 12:70. 10.1186/s13073-020-00767-w

Qin L, Xiong B, Luo C, Guo ZM, Hao P, Su J, Nan P, Feng Y, Shi YX, Yu XJ, Luo XM, Chen KX, Shen X, Shen JH, Zou JP, Zhao GP, Shi TL, He WZ, Zhong Y, Jiang HL, and Li YX. 2003. Identification of probable genomic packaging signal sequence from SARS-CoV genome by bioinformatics analysis. *Acta Pharmacol Sin* 24:489-496.

Qiu LW, Tang HW, Wang YD, Liao JE, Hao W, Wen K, He XM, and Che XY. 2005. [Development and application of triple antibodies-based sandwich ELISA for detecting nucleocapsid protein of SARS-associated coronavirus]. *Zhonghua Liu Xing Bing Xue Za Zhi* 26:277-281.

Robson B. 2020. Computers and viral diseases. Preliminary bioinformatics studies on the design of a synthetic vaccine and a preventative peptidomimetic antagonist against the SARS-CoV-2 (2019-nCoV, COVID-19) coronavirus. *Comput Biol Med* 119:103670. 10.1016/j.compbiomed.2020.103670

Rothe C, Schunk M, Sothmann P, Bretzel G, Froeschl G, Wallrauch C, Zimmer T, Thiel V, Janke C, Guggemos W, Seilmaier M, Drosten C, Vollmar P, Zwirglmaier K, Zange S, Wolfel R, and Hoelscher M. 2020. Transmission of 2019-nCoV Infection from an Asymptomatic Contact in Germany. *N Engl J Med* 382:970-971. 10.1056/NEJMc2001468

Saha R, Ghosh P, and Burra V. 2021. Designing a next generation multi-epitope based peptide vaccine candidate against SARS-CoV-2 using computational approaches. *3 Biotech* 11:47. 10.1007/s13205-020-02574-x

Saha S, and Raghava GP. 2006. Prediction of continuous B-cell epitopes in an antigen using recurrent neural network. *Proteins* 65:40-48. 10.1002/prot.21078

Sanchez CM, Izeta A, Sanchez-Morgado JM, Alonso S, Sola I, Balasch M, Plana-Duran J, and Enjuanes L. 1999.

Targeted recombination demonstrates that the spike gene of transmissible gastroenteritis coronavirus is a determinant of its enteric tropism and virulence. *J Virol* 73:7607-7618.

Shajahan A, Supekar NT, Gleinich AS, and Azadi P. 2020. Deducing the N- and O- glycosylation profile of the spike protein of novel coronavirus SARS-CoV-2. *Glycobiology*. 10.1093/glycob/cwaa042

Shaman J, and Galanti M. 2020. Will SARS-CoV-2 become endemic? *Science* 370:527-529. 10.1126/science.abe5960

Shang J, Ye G, Shi K, Wan Y, Luo C, Aihara H, Geng Q, Auerbach A, and Li F. 2020. Structural basis of receptor recognition by SARS-CoV-2. *Nature*. 10.1038/s41586-020-2179-y

Shen X, Xue JH, Yu CY, Luo HB, Qin L, Yu XJ, Chen J, Chen LL, Xiong B, Yue LD, Cai JH, Shen JH, Luo XM, Chen KX, Shi TL, Li YX, Hu GX, and Jiang HL. 2003. Small envelope protein E of SARS: cloning, expression, purification, CD determination, and bioinformatics analysis. *Acta Pharmacol Sin* 24:505-511.

Shulman Z, Gitlin A, Weinstein J, Lainez B, Esplugues E, Flavell R, Craft J, and Nussenzweig M. 2014. Dynamic signaling by T follicular helper cells during germinal center B cell selection. *Science (New York, NY)* 345:1058-1062. 10.1126/science.1257861

Sievers F, Wilm A, Dineen D, Gibson TJ, Karplus K, Li W, Lopez R, McWilliam H, Remmert M, Soding J, Thompson JD, and Higgins DG. 2011. Fast, scalable generation of high-quality protein multiple sequence alignments using Clustal Omega. *Mol Syst Biol* 7:539. 10.1038/msb.2011.75

Sohail M, Ahmed S, Quadeer A, and McKay M. 2021. In silico T cell epitope identification for SARS-CoV-2: Progress and perspectives. *Advanced drug delivery reviews*. 10.1016/j.addr.2021.01.007

Su S, Wong G, Shi W, Liu J, Lai ACK, Zhou J, Liu W, Bi Y, and Gao GF. 2016. Epidemiology, Genetic Recombination, and Pathogenesis of Coronaviruses. *Trends Microbiol* 24:490-502. 10.1016/j.tim.2016.03.003

Sunwoo HH, Palaniyappan A, Ganguly A, Bhatnagar PK, Das D, El-Kadi AO, and Suresh MR. 2013. Quantitative and sensitive detection of the SARS-CoV spike protein using bispecific monoclonal antibody-based enzyme-linked immunoassay. *J Virol Methods* 187:72-78. 10.1016/j.jviromet.2012.09.006

Tan YJ, Goh PY, Fielding BC, Shen S, Chou CF, Fu JL, Leong HN, Leo YS, Ooi EE, Ling AE, Lim SG, and Hong W. 2004. Profiles of antibody responses against severe acute respiratory syndrome coronavirus recombinant proteins and their potential use as diagnostic markers. *Clin Diagn Lab Immunol* 11:362-371. 10.1128/cdli.11.2.362-371.2004

Tang MS, Hock KG, Logsdon NM, Hayes JE, Gronowski AM, Anderson NW, and Farnsworth CW. 2020. Clinical Performance of Two SARS-CoV-2 Serologic Assays. *Clin Chem*. 10.1093/clinchem/hvaa120

Tegally H, Wilkinson E, Giovanetti M, Iranzadeh A, Fonseca V, Giandhari J, Doolabh D, Pillay S, San EJ, Msomi N, Mlisana K, von Gottberg A, Walaza S, Allam M, Ismail A, Mohale T, Glass AJ, Engelbrecht S, Van Zyl G, Preiser W, Petruccione F, Sigal A, Hardie D, Marais G, Hsiao M, Korsman S, Davies M-A, Tyers L, Mudau I, York D, Maslo C, Goedhals D, Abrahams S, Laguda-Akingba O, Alisoltani-Dehkordi A, Godzik A, Wibmer CK, Sewell BT, Lourenço J, Alcantara LCJ, Pond SLK, Weaver S, Martin D, Lessells RJ, Bhiman JN, Williamson C, and de Oliveira T. 2020. Emergence and rapid spread of a new severe acute respiratory syndrome-related coronavirus 2 (SARS-CoV-2) lineage with multiple spike mutations in South Africa. *medRxiv* 10.1101/2020.12.21.20248640

Thabet L, Mhalla S, Naija H, Jaoua MA, Hannachi N, Fki-Berrajah L, Toumi A, and Karray-Hakim H. 2020. SARS-CoV-2 infection virological diagnosis. *Tunis Med* 98:304-308.

Trolle T, Metushi IG, Greenbaum JA, Kim Y, Sidney J, Lund O, Sette A, Peters B, and Nielsen M. 2015. Automated benchmarking of peptide-MHC class I binding predictions. *Bioinformatics* 31:2174-2181.

10.1093/bioinformatics/btv123

Vita R, Mahajan S, Overton JA, Dhanda SK, Martini S, Cantrell JR, Wheeler DK, Sette A, and Peters B. 2019. The Immune Epitope Database (IEDB): 2018 update. *Nucleic Acids Res* 47:D339-d343. 10.1093/nar/gky1006

Walls AC, Xiong X, Park YJ, Tortorici MA, Snijder J, Quispe J, Cameroni E, Gopal R, Dai M, Lanzavecchia A, Zambon M, Rey FA, Corti D, and Veesler D. 2019. Unexpected Receptor Functional Mimicry Elucidates Activation of Coronavirus Fusion. *Cell* 176:1026-1039.e1015. 10.1016/j.cell.2018.12.028

Wang P, Sidney J, Kim Y, Sette A, Lund O, Nielsen M, and Peters B. 2010. Peptide binding predictions for HLA DR, DP and DQ molecules. *BMC Bioinformatics* 11:568. 10.1186/1471-2105-11-568

Wang R, Hozumi Y, Yin C, and Wei G-W. 2020a. Mutations on COVID-19 diagnostic targets. *Genomics* 112:5204-5213. 10.1016/j.ygeno.2020.09.028

Wang R, Hozumi Y, Yin C, and Wei GW. 2020b. Decoding SARS-CoV-2 Transmission and Evolution and Ramifications for COVID-19 Diagnosis, Vaccine, and Medicine. *J Chem Inf Model*. 10.1021/acs.jcim.0c00501

Wilkins MR, Gasteiger E, Bairoch A, Sanchez JC, Williams KL, Appel RD, and Hochstrasser DF. 1999. Protein identification and analysis tools in the ExPASy server. *Methods Mol Biol* 112:531-552. 10.1385/1-59259-584-7:531

Woo PC, Lau SK, Wong BH, Tsoi HW, Fung AM, Kao RY, Chan KH, Peiris JS, and Yuen KY. 2005. Differential sensitivities of severe acute respiratory syndrome (SARS) coronavirus spike polypeptide enzyme-linked immunosorbent assay (ELISA) and SARS coronavirus nucleocapsid protein ELISA for serodiagnosis of SARS coronavirus pneumonia. *J Clin Microbiol* 43:3054-3058. 10.1128/JCM.43.7.3054-3058.2005

Yan Y, Chang L, and Wang L. 2020. Laboratory testing of SARS-CoV, MERS-CoV, and SARS-CoV-2 (2019-nCoV): Current status, challenges, and countermeasures. *Rev Med Virol* 30:e2106. 10.1002/rmv.2106

Yuan S, Chan HCS, Filipek S, and Vogel H. 2016. PyMOL and Inkscape Bridge the Data and the Data Visualization. *Structure* 24:2041-2042. 10.1016/j.str.2016.11.012

Zhan SH, Deverman BE, and Chan YA. 2020. 10.1101/2020.05.01.073262

Zhang L, Udaka K, Mamitsuka H, and Zhu S. 2012. Toward more accurate pan-specific MHC-peptide binding prediction: a review of current methods and tools. *Brief Bioinform* 13:350-364. 10.1093/bib/bbr060

Zheng K, Bantog C, and Bayer R. 2011. The impact of glycosylation on monoclonal antibody conformation and stability. *MAbs* 3:568-576. 10.4161/mabs.3.6.17922

Figure 1

Work flow chart

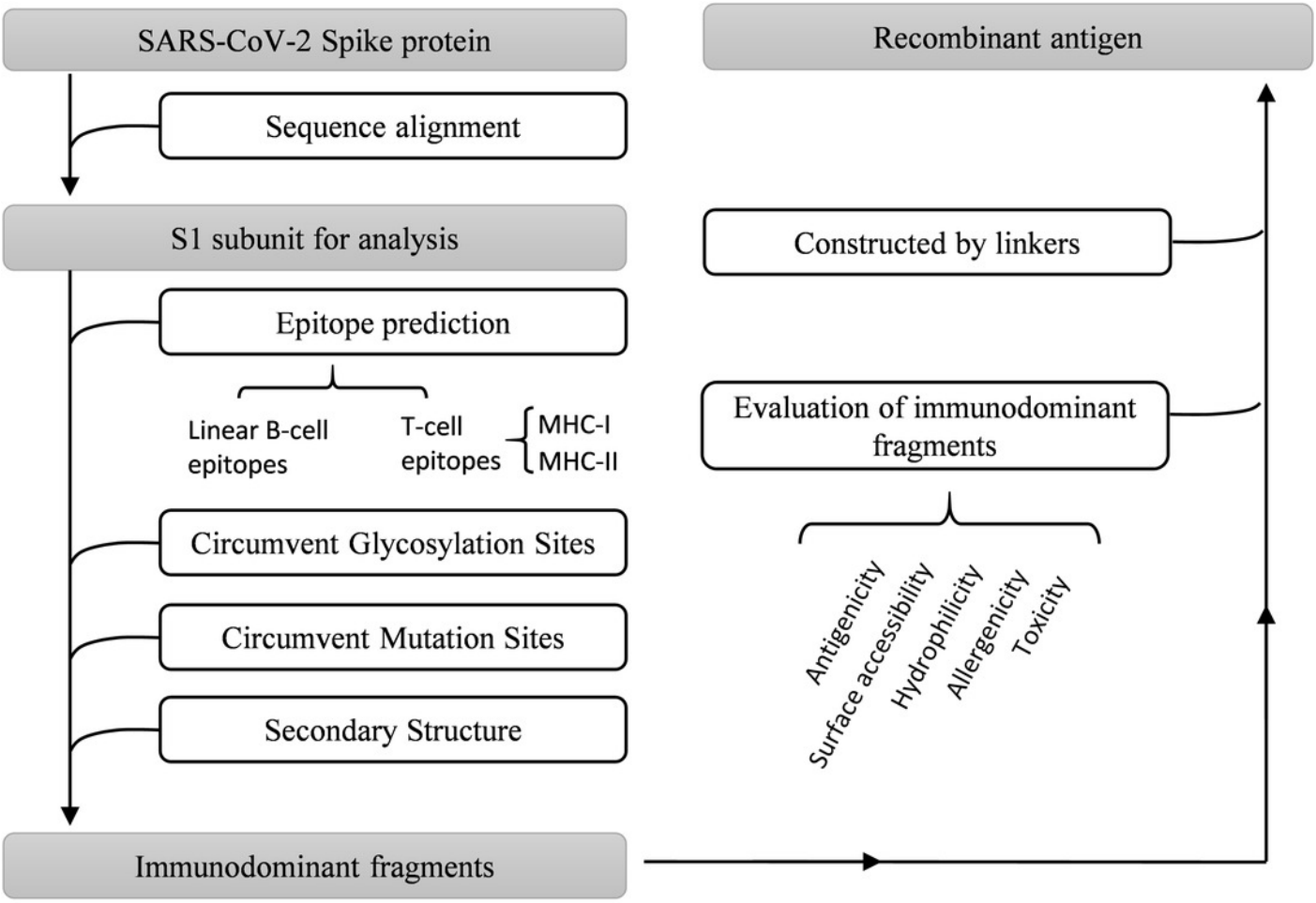

Figure 2

Sequence alignment results of spike protein

A. Accession IDs and sequence identities of selected coronavirus spike protein. B. Phylogenetic tree of spike proteins among selected coronavirus. C. Sequence identity of major domains in spike protein between SARS-CoV-2 and SARS-CoV. D. Sequence identity of domains in SARS-CoV-2 and SARS-CoV reflected by colors. From red to green, the color changing represents the sequence identity from high to low.

A

Virus	Accession ID	Identity compared to SARS-CoV-2(%)
SARS-CoV-2	QIC53213.1	100
SARS-COV	ABD72968.1	77.46
MERS-COV	QBM11748.1	32.04
HCoV-NL63	YP_003767.1	25.57
HCoV-229E	AWH62679.1	26.90
HCoV-OC43	AIX10763.1	30.92
HCoV-HKU1	AMN88694.1	29.92

B

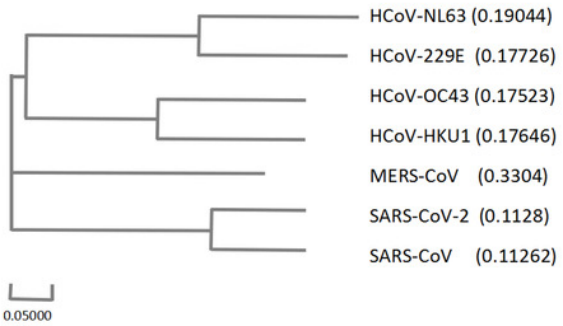

C

Domains	Length	Identity (%)
Spike protein	1277	76.4
S1 subunit	68.9	64.6
NTD	304	50.0
RBM	71	49.3
RBD	222	73.0
S2 subunit	588	90.0

D

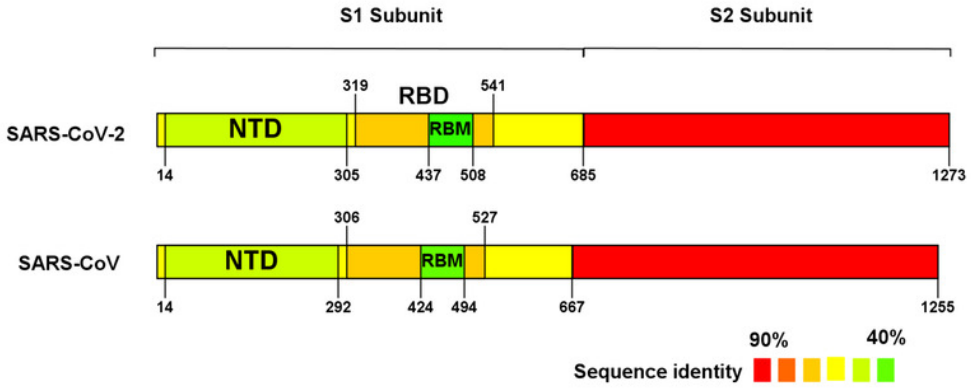

Figure 3

Preliminary immunodominant fragments based on B-cell epitope prediction results

The black squares represent epitopes predicted by ABCpred server, the black frames represent epitopes predicted by Bepipred v2.0 server, and the black lines with numbers on both ends represent the preliminary candidate immunodominant fragments.

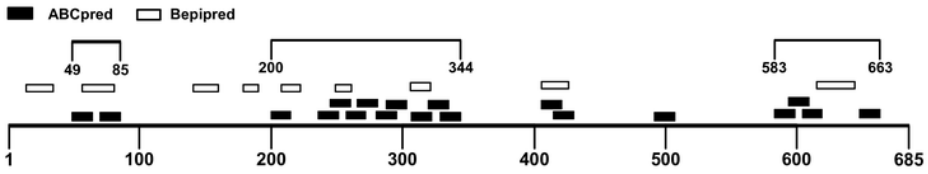

Figure 4

Adjusted candidate immunodominant fragments according to MHC-II T-cell epitope prediction results

The black squares represent epitopes predicted by ABCpred server, and the black frames represent epitopes predicted by Bepipred v2.0 server. The red frames denote MHC-II binding epitopes. The black lines with numbers on both ends represent the adjusted candidate fragments.

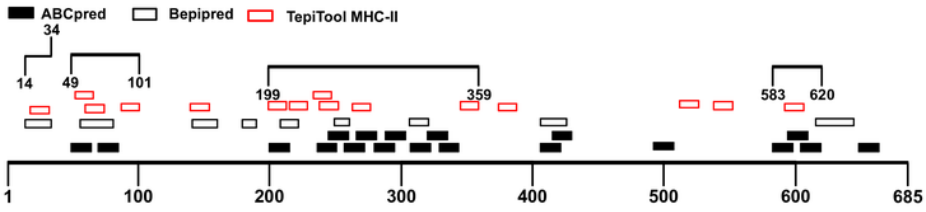

Figure 5

The epitopes and glycosylation sites on the selected immunodominant fragments

The black squares represent epitopes predicted by ABCpred server, and the black frames represent epitopes predicted by Bepipred v2.0 server. The red squares represent MHC-I binding epitopes, and the red frames represent MHC-II binding epitopes. The grey squares means occupied glycosylation sites contained in the selected fragments.

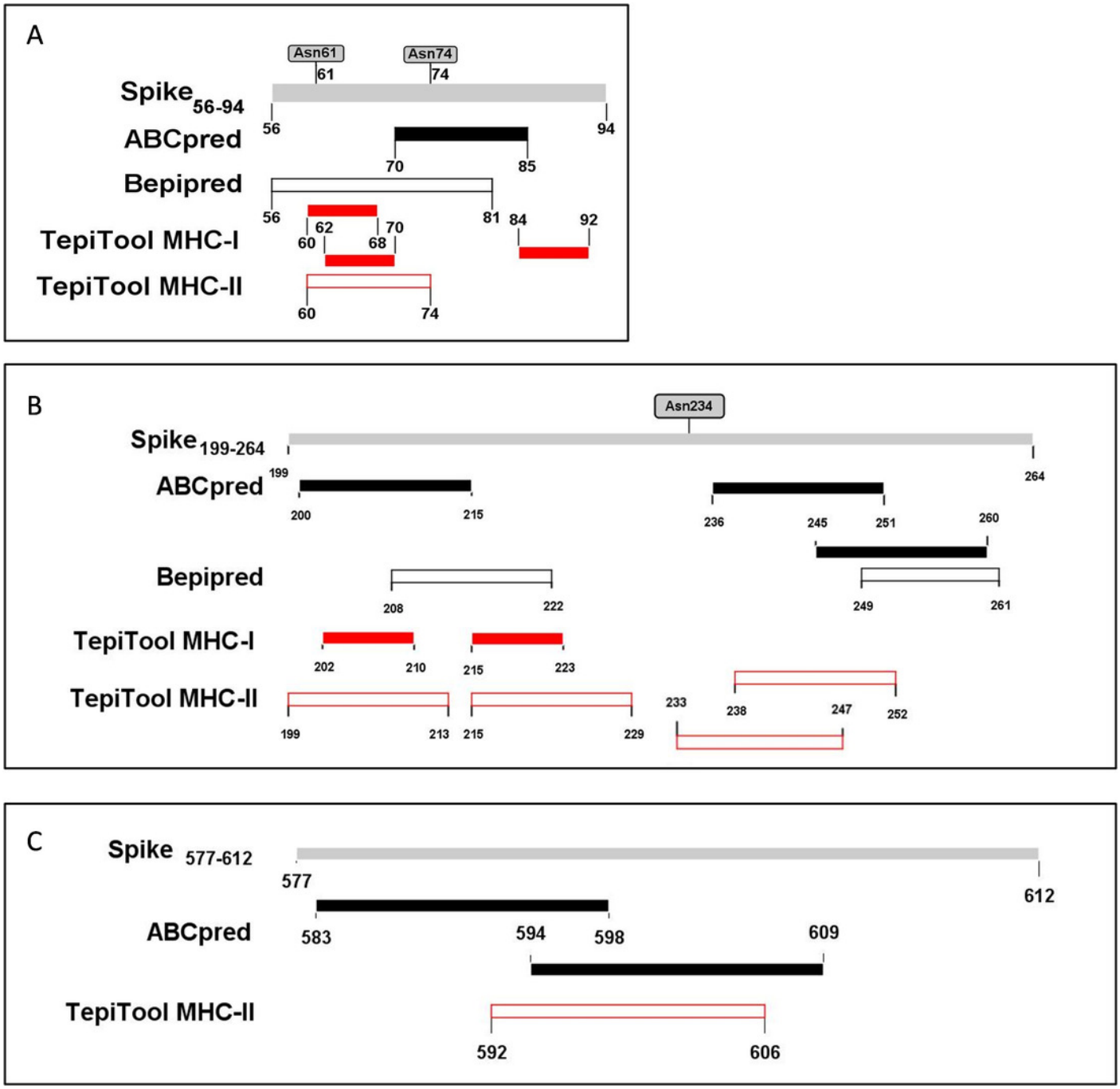
A
Asn61
61
Asn74
74
Spike 56-94
56
94
ABCpred
70
85
Bepipred
56
81
TepiTool MHC-I
62
70
60
68
84
92
TepiTool MHC-II
60
74
B
Asn234
Spike 199-264
199
264
ABCpred
200
215
236
245
251
260
Bepipred
208
222
249
261
TepiTool MHC-I
202
210
215
223
TepiTool MHC-II
199
213
215
229
233
238
247
252
C
Spike 577-612
577
612
ABCpred
583
594
598
609
TepiTool MHC-II
592
606

Figure 6

Selected immunodominant fragments presented as spheres in the trimer structure of spike protein viewed by PyMOL

Selected fragments were presented as red spheres, green cartoons denote unselected sections. A, B, and C denote fragments Spike56-94, Spike199-264, and Spike577-612 respectively.

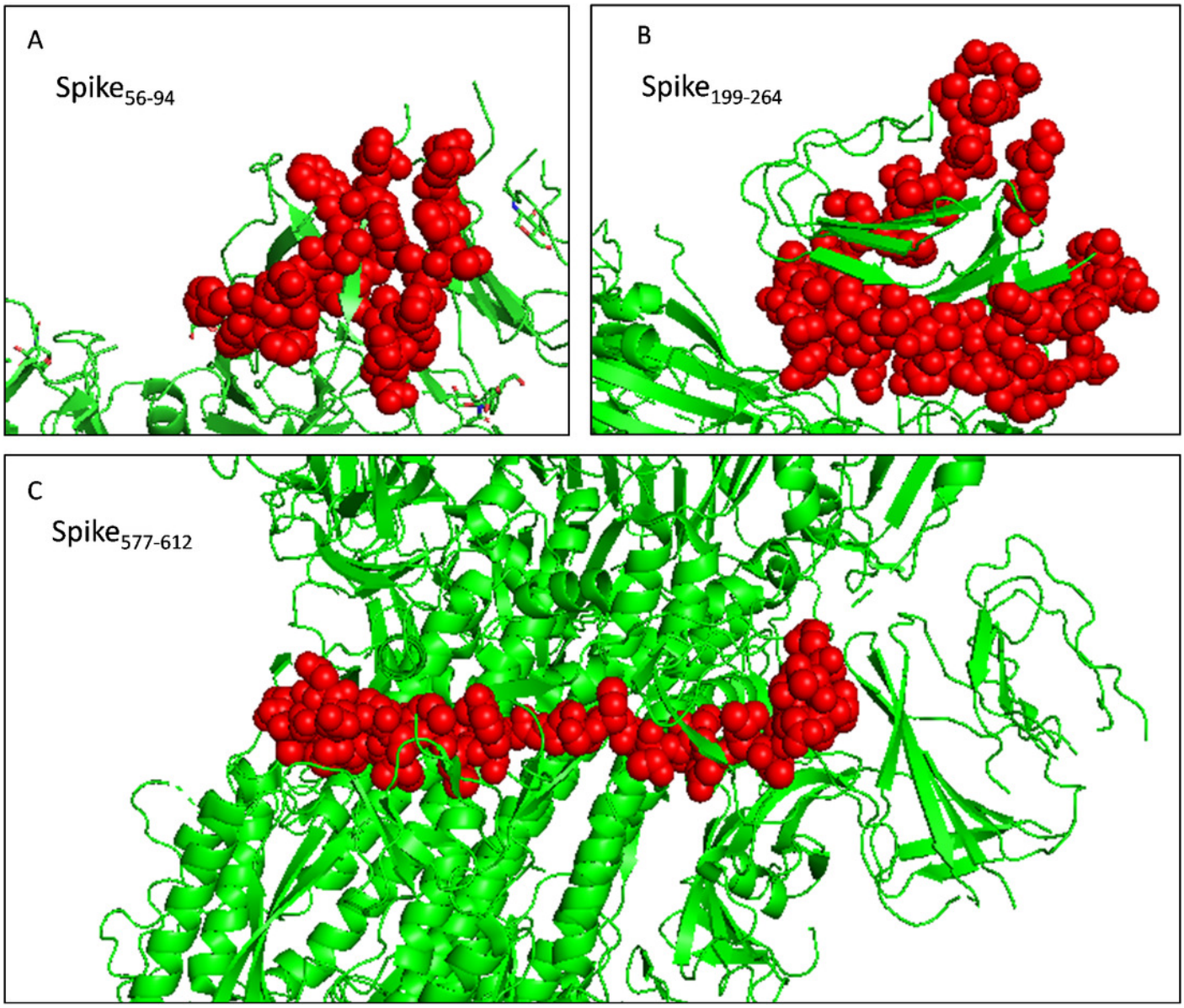

Figure 7

A schematic diagram of recombinant peptide composed of selected fragments and a PADRE epitope.

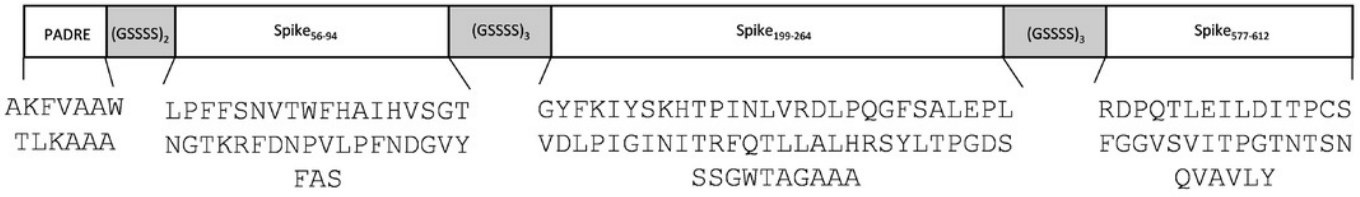

Table 1(on next page)

Linear B-cell epitopes predicted by ABCpred and BepiPred v2.0 with antigenicity score exceed the threshold value

1

Tools	Position	Sequence	Length	Antigenicity (cut off≥0.4)
ABCpred	583-598	EILDITPCSFGGVSVI	16	1.3971
	406-421	EVRQIAPGQTGKIADY	16	1.3837
	415-430	TGKIADYNYKLPDDFT	16	0.9642
	648-663	GCLIGAEHVNNSYECD	16	0.848
	288-303	AVDCALDPLSETKCTL	16	0.7905
	604-619	TSNQVAVLYQDVNCTE	16	0.7593
	307-322	TVEKGIYQTSNFRVQP	16	0.6733
	200-215	YFKIYSKHTPINLVRD	16	0.657
	257-272	GWTAGAAAYYVGYLQP	16	0.621
	329-344	FPNITNLCPFGEVFNA	16	0.6058
	245-260	HRSYLTPGDSSSGWTA	16	0.6017
	280-295	NENGTITDAVDCALDP	16	0.5804
	49-64	HSTQDLFLPFFSNVTW	16	0.5305
	492-507	LQSYGFQPTNGVGYQP	16	0.5258
	70-85	VSGTNGTKRFDNPVLP	16	0.5162
	236-251	TRFQTLLALHRSYLTP	16	0.5115
	266-281	YVGYLQPRTFLLKYNE	16	0.5108
	594-609	GVSVITPGTNTSNQVA	16	0.4651
	320-335	VQPTESIVRFPNITNL	16	0.4454
Bepipred v2.0	179-190	LEGKQGNFKNLR	12	1.1188
	404-426	GDEVRQIAPGQTGKIADYNYKLP	23	1.1017
	14-34	QCVNLTTRTQLPPAYTNSFTR	21	0.7594
	56-81	LPFFSNVTWFHAIHVSGTNGTKRFDN	26	0.6041
	208-222	TPINLVRDLPQGFSA	15	0.5531
	141-160	LGVYYHKNNKSWMESEFRVY	20	0.5308
	249-261	LTPGDSSSGWTAG	13	0.495
	306-321	FTVEKGIYQTSNFRVQ	16	0.4361
	615-644	VNCTEVPVAIHADQLTPTWRVYSTGSNVFQ	30	0.4259

Table 2(on next page)

Details of epitopes in the preliminary immunodominant fragments selected according to linear B-cell epitope prediction results.

1

Regions	Epitope predicted by ABCpred			Epitope predicted by Bepipred v2.0		
	Position	Sequence	Antigenicity	Position	Sequence	Antigenicity
49-85	49-64	HSTQDLFLPFFSNVTW	0.5305	56-81	LPFFSNVTWFHAIHV SGTNGTKRFDN	0.6041
	70-85	VSGTNGTKRFDNPVLP	0.5162			
200-344	200-215	YFKIYSKHTPINLVRD	0.6570	208-222	TPINLVRDLPQGFSA	0.5531
	236-251	TRFQTLLALHRSYLTP	0.5115	249-261	LTPGDSSSGWTAG	0.4950
	245-260	HRSYLTPGDSSSGWTA	0.6017			
	257-272	GWTAGAAAYYVGYLQP	0.6210			
	266-281	YVGYLQPRTFLLKYNE	0.5108			
	280-295	NENGTITDAVDCALDP	0.5804			
	288-303	AVDCALDPLSETKCTL	0.7905	306-321	FTVEKGIYQTSNFRV Q	0.4361
	307-322	TVEKGIYQTSNFRVQP	0.6733			
	320-335	VQPTESIVRFPNITNL	0.4454			
	329-344	FPNITNLCPFGEVFNA	0.6058			
	415-430	TGKIADYNYKLPDDFT	0.9642			
583-663	583-598	EILDITPCSFGGVSVI	1.3971	615-644	VNCTEVPVAIHADQL TPTWRVYSTGSNVFQ	0.4259
	594-609	GVSVITPGTNTSNQVA	0.4651			
	604-619	TSNQVAVLYQDVNCTE	0.7593			
	648-663	GCLIGAEHVNNSYECD	0.8480			

Table 3(on next page)

MHC-II and MHC-I binding epitopes predicted by TepiTool server with antigenicity score exceed threshold value

Type	Position	Sequence	Length	Allele	Core (smm-align)	Core (nn-align)	Percentile Rank	Antigenicity (cut off≥0.4
MHC-II binding	538-552	CVNFNFNGLTGTGVL	15	H2-IAb	FNFNGLTGT	FNFNGLTGT	8.55	1.3281
	374-388	FSTFKCYGVSPTKLN	15	H2-IAb	FKCYGVSPT	YGVSPTKLN	6.45	1.0042
	199-213	GYFKIYSKHTPINLV	15	H2-Iab	KIYSKHTPI	YSKHTPINL	6.9	0.9278
	18-32	LTTRTQLPPAYTNSF	15	H2-IAb	TRTQLPPAY	TRTQLPPAY	9.9	0.79
	60-74	SNVTWFHAIHVSGTN	15	H2-IAb	VTWFHAIHV	TWFHAIHVS	9.1	0.7044
	263-277	AAYYVGYLQPRTFLL	15	H2-IAb	VGYLQPRTF	VGYLQPRTF	8.75	0.6073
	592-606	FGGVSVITPGTNTSN	15	H2-IAb	VITPGTNTS	VSVITPGTN	6	0.5825
	238-252	FQTLLALHRSYLTPG	15	H2-IEd	TLLALHRSY	TLLALHRSY	9.85	0.5789
	345-359	TRFASVYAWNRKRIS	15	H2-IAb	FASVYAWNR	YAWNRKRIS	7.45	0.4963
	215-229	DLPQGFSALEPLVDL	15	H2-IAb	FSALEPLVD	FSALEPLVD	6.05	0.4812
	140-154	FLGVYYHKNNKSWME	15	H2-IEd	GVYYHKNNK	YYHKNNKSW	6.4	0.4793
	512-526	VLSFELLHAPATVCG	15	H2-IAb	FELLHAPAT	FELLHAPAT	2.9	0.4784
	87-101	NDGVYFASTEKSNII	15	H2-Iab	YFASTEKSN	VYFASTEKS	6.85	0.4277
	52-66	QDLFLPFFSNVTWFH	15	H2-IAb	FLPFFSNVT	FLPFFSNVT	2.95	0.4159
	233-247	INITRFQTLLALHRS	15	H2-IAd	ITRFQTLLA	ITRFQTLLA	1.9	0.4118
MHC-I binding	643-651	FQTRAGCLI	9	H-2-Kk			0.6	1.7332
	612-620	YQDVNCTEV	9	H-2-Db			0.4	1.6172
	539-547	VNFNFNGLT	9	H-2-Kb			0.47	1.5069
	503-511	VGYQPYRVV	9	H-2-Kb			0.47	1.4383
	379-387	CYGVSPTKL	9	H-2-Kd			0.3	1.4263
	16-24	VNLTTRTQL	9	H-2-Kb			0.86	1.3468
	510-518	VVVLSFELL	9	H-2-Kb			0.43	1.0909
	202-210	KIYSKHTPI	9	H-2-Kb			0.27	0.7455
	168-176	FEYVSQPFL	9	H-2-Kk			0.5	0.6324
	268-276	GYLQPRTFL	9	H-2-Kd			0.2	0.6082
	505-513	YQPYRVVVL	9	H-2-Dd			0.3	0.5964
	488-496	CYFPLQSYG	9	H-2-Kd			0.64	0.578
	215-223	DLPQGFSAL	9	H-2-Dd			0.69	0.5622
	342-350	FNATRFASV	9	H-2-Kb			0.56	0.5609
	84-92	LPFNDGVYF	9	H-2-Ld			0.21	0.5593
	484-492	EGFNCYFPL	9	H-2-Kb			0.84	0.5453
	62-70	VTWFHAIHV	9	H-2-Kb			0.61	0.5426
	489-497	YFPLQSYGF	9	H-2-Dd			0.8	0.5107
	350-358	VYAWNRKRI	9	H-2-Kd			0.7	0.5003
	60-68	SNVTWFHAI	9	H-2-Kb			0.82	0.4892
	262-270	AAAYYVGYL	9	H-2-Kb			0.98	0.4605

1

Table 4(on next page)

Details of candidate immunodominant fragments adjusted according to the MHC-II binding T-cell epitopes prediction results.

1

Regions	Linear B-cell epitopes				MHC-II binding epitopes		
	Tools	Position	Sequence	Antigenicity	Position	Sequence	Antigenicity
14-34	Bepipred v2.0	14-34	QCVNLTTRTQLPPAYTN SFTR	0.7594	18-32	LTTRTQLPPAYTNSF	0.7900
49-101	Bepipred v2.0	56-81	LPFFSNVTWFHAIHVSG TNGTKRFDN	0.6041	52-66	QDLFLPFFSNVTWFH	0.4159
	ABCpred	49-64	HSTQDLFLPFFSNVTW	0.5305	60-74	SNVTWFHAIHVSGTN	0.7044
	ABCpred	70-85	VSGTNGTKRFDNPVLP	0.5162	87-101	NDGVYFASTEKSNII	0.4277
199-359	Bepipred v2.0	208-222	TPINLVRDLPQGFSA	0.5531	199-213	GYFKIYSKHTPINLV	0.9278
		249-261	LTPGDSSSGWTAG	0.4950			
		306-321	FTVEKGIYQTSNFRVQ	0.4361			
	ABCpred	200-215	YFKIYSKHTPINLVRD	0.6570			
		236-251	TRFQTLLALHRSYLTP	0.5115	215-229	DLPQGFSALEPLVDL	0.4812
		245-260	HRSYLTPGDSSSGWTA	0.6017			
		257-272	GWTAGAAAYYVGYLQP	0.6210	233-247	INITRFQTLLALHRS	0.4118
		266-281	YVGYLQPRTFLLKYNE	0.5108			
		280-295	NENGTITDAVDCALDP	0.5804	238-252	FQTLLALHRSYLTPG	0.5789
		288-303	AVDCALDPLSETKCTL	0.7905			
		307-322	TVEKGIYQTSNFRVQP	0.6733	263-277	AAYYVGYLQPRTFLL	0.6073
		320-335	VQPTESIVRFPNITNL	0.4454			
		329-344	FPNITNLCPFGEVFNA	0.6058			
					345-359	TRFASVYAWNRKRIS	0.4963
583-620	ABCpred	583-598	EILDITPCSFGGVSVI	1.3971	592-606	FGGVSVITPGTNTSN	0.5825
		594-609	GVSVITPGTNTSNQVA	0.4651			
		604-619	TSNQVAVLYQDVNCTE	0.7593			

Table 5(on next page)

Significant features of the selected immunodominant fragments.

The sequences marked as bold and italic in the table represent amino acids with hydrophilicity and surface accessibility respectively

Fragments	$Spike_{56-94}$	$Spike_{199-264}$	$Spike_{577-612}$
Length(aa)	39	66	36
Sequence	LPFFSNVTWFHAIHVS GTNGTKRFDNPVLPF NDGVYFAS	GYFKIYSKHTPINLVRDLPQGFSALEPLVD LPIGINITRFQTLLALHRSYLTPGDSSSGW TAGAAA	RDPQTLEILDITPCSFG GVSVITPGTNTSNQVA VLY
Antigenicity	0.4590	0.5774	0.9127
Domain	S1(NTD)	S1(NTD)	S1
Hydrophilicity fragments	LPFFSNVTWFHAIH***V***S ***GTNGTKRFDNPVLP***F NDGV***YFAS***	***GY***F***KIYSKHTPIN***LV***RD***L***PQ***GF***S***ALEPLVD LPIGINIT***R***FQTLLALHRS***YLTPGDSSSGWT*** AGAAA	***RDPQTL***EILDITPCSFG GVSVITPG***TNTSN***QVA ***V***LY
Surface Accessibility fragments	LP***FFSN***VTWFHAI***H***V ***SGTNGTKR***F***D***N***P***VL***P***F ***ND***GVYFAS	G***Y***FKIYSK***HTPINLVRD***L***PQGF***SAL***E***PLV ***D***LPIGI***N***I***TR***FQTLLALHRS***YLTPGDSSS***G WTAGAAA	***R***D***PQT***L***E***IL***DITPC***SFG*** GVSVIT***PGTNTSNQ***VA VLY
Toxicity	Non-toxin	Non-toxin	Non-toxin
Allergenicity	non-allergen	non-allergen	probable allergen

1

Table 6(on next page)

The structure and antigenicity of final recombinant peptides

Final construct	PAN DR + $(GGGGS)_2$ + $Spike_{56-94}$ +$(GGGGS)_3$ + $Spike_{199-264}$ +$(GGGGS)_3$ + $Spike_{577-612}$
Sequence	AKFVAAWTLKAAAGGGGSGGGGSLPFFSNVTWFHAIHVSGTNGTKRFDNPVLPFNDGVYFASGGGGSGGGGS GGGGSGYFKIYSKHTPINLVRDLPQGFSALEPLVDLPIGINITRFQTLLALHRSYLTPGDSSSGWTAGAAAG GGGSGGGGSGGGGSRDPQTLEILDITPCSFGGVSVITPGTNTSNQVAVLY
Antigenicity	0.5690

1